Impulsively Excited Gravitational Quantum States: Echoes and Time-Resolved Spectroscopy

I. Tutunnikov,[1] K. V. Rajitha,[1] A. Yu. Voronin,[2,*] V. V. Nesvizhevsky,[3,†] and I. Sh. Averbukh[1,‡]
[1]*AMOS and Department of Chemical and Biological Physics, The Weizmann Institute of Science, Rehovot 7610001, Israel*
[2]*P. N. Lebedev Physical Institute, 53 Leninsky Prospect, Moscow Ru-119333, Russia*
[3]*Institut Max von Laue-Paul Langevin (ILL), 71 avenue des Martyrs, F-38042 Grenoble, France*

(Received 26 September 2020; revised 18 December 2020; accepted 29 March 2021; published 30 April 2021)

We theoretically study an impulsively excited quantum bouncer (QB)—a particle bouncing off a surface in the presence of gravity. A pair of time-delayed pulsed excitations is shown to induce a wave-packet echo effect—a partial rephasing of the QB wave function appearing at twice the delay between pulses. In addition, an appropriately chosen observable [here, the population of the ground gravitational quantum state (GQS)] recorded as a function of the delay is shown to contain the transition frequencies between the GQSs, their populations, and partial phase information about the wave-packet quantum amplitudes. The wave-packet echo effect is a promising candidate method for precision studies of GQSs of ultracold neutrons, atoms, and antiatoms confined in closed gravitational traps.

DOI: 10.1103/PhysRevLett.126.170403

Introduction.—In the last decades, massive quantum particle bouncing off a surface under the influence of gravity turned from being an issue of textbooks and pedagogical essays [1–4] into a subject of precision experiments on atom-optics gravitational cavities [5,6] and physics of ultracold neutrons (UCNs) [7]. The observation of gravitational quantum states (GQSs) [8–11] and whispering gallery states [12,13] of neutrons (n) fueled a vast research in this area which, among other goals, aims to the search for new fundamental short-range interactions and physics beyond the Standard Model, as well as verification of weak equivalence principle in the quantum regime (see, e.g., the introduction of [14], and references therein).

Cold atoms and antiatoms can also bounce on surfaces and form GQSs [15] due to the quantum reflection from a rapidly changing attractive van der Waals (Casimir-Polder) surface potential (see, e.g., [16] and references therein). In contrast to the extremely precise measurements of gravitational properties of matter [17–19], the best constraint [20] for the gravitational mass (acceleration) of antimatter does not allow us to even define the sign of acceleration. Several collaborations perform experiments at CERN [21–23] aiming to improve the accuracy. The GQSs method seems to promise the best accuracy for antihydrogen atoms ($\bar{\mathrm{H}}$) [24].

Resonant spectroscopy of neutron GQSs was proposed in [25], measured using periodic excitation of quantum bouncers (QBs) by mechanical vibrations of the surface [26–30], and is being implemented using a periodically changing magnetic field gradient [31,32]. Spatial distribution of GQSs of n was measured with micron resolution [33]. For bouncing $\bar{\mathrm{H}}$ atoms, resonant spectroscopy [34,35] and interferometry [24,36,37] approaches have been developed.

Here, we study the physics of impulsively excited QBs, and consider two example excitations: (i) by applying a pulsed magnetic field gradient interacting with the QB's magnetic dipole moment, and (ii) by a jolt caused by an impulsive shake of the surface. Short laser pulses have been widely used for time-resolved molecular spectroscopy, however, the related aspects of the GQS spectroscopy are unexplored yet. A spectacular effect in the dynamics of kick-excited nonlinear systems is the echo phenomenon first discovered by E. Hahn in spin systems [38,39] (spin echo). Since then, various types of echoes have been observed, including photon echoes [40,41], cyclotron echoes [42], plasma-wave echoes [43], neutron spin echoes [44], cold atom echoes in optical traps [45–47], echoes in particle accelerators [48–52], and more recently, alignment and orientation echoes in molecular gases [53–61]. In these examples, an echo appears in inhomogeneous ensembles of many particles evolving at different frequencies. Echoes were also observed in single quantum objects: in a single mode of quantized electromagnetic field interacting with atoms passing through a cavity [62,63] and in single vibrationally excited molecules [64].

In the first part of this Letter, we demonstrate, for the first time, that highly nonlinear dynamics of the classical particle bouncing over an impenetrable reflective surface favors observation of the echo in single quantum bouncers. Then, we explore the response of a QB to a pair of time-delayed kicks, and analyze its dependence on the delay between kicks. The population of the ground GQS as a function of the delay is shown to contain the transition frequencies between the populated GQSs, as well as partial phase information about the QB wave packet. This paves

 © 2021 American Physical Society

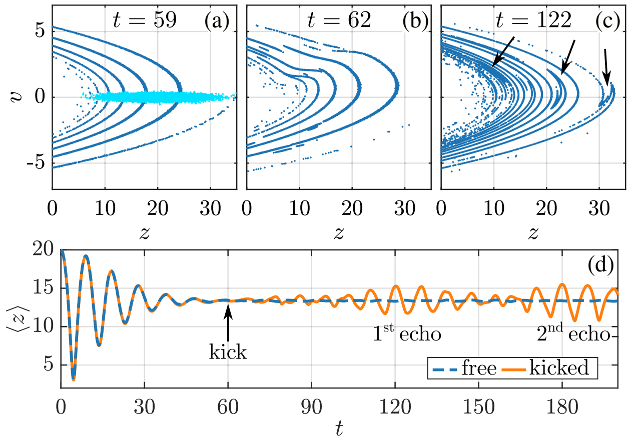

FIG. 1. Phase space analysis. $N = 2 \times 10^4$ particles bounce on a surface, and kicked at $t = t_k = 60$. Kick parameters: $a_k = 0.5$ (e.g., for neutrons: $|\boldsymbol{\mu}| = 60.3$ neV/T, $\hat{\beta} \approx 0.8$ T/m), $\sigma_k = 0.5$. Initial distribution [light blue, (a)] parameters: $\mu_z = 20.0$, $\mu_v = 0.0$, $\sigma_z = 4$, $\sigma_v = 1/8$. (a) In blue—filamented phase space before the kick. (b) Shortly after the kick. (c) Close to echo event, at $t \approx 2t_k$. Arrows point at the tips (see the text). (d) Average position.

the way for a new kind of time-resolved GQS spectroscopy which has a number of advantages. It doesn't require fine tuning of the excitation frequency to a specific resonance between the GQSs, and it eliminates some frequency shifts characteristic of the resonant GQS spectroscopy [32].

Free quantum bouncer.—The vertical motion of the QB (along the Z axis) is quantized and decoupled from the motion along the X and Y axes. The eigenfunctions ψ_i and energies E_i of the QB of mass m are found from

$$H_g\psi_i = -\frac{\hbar^2}{2m}\frac{\partial^2\psi_i}{\partial z^2} + mgz\psi_i = E_i\psi_i, \qquad (1)$$

where g is the gravitational acceleration, and z is the vertical position. Inertial and gravitational masses are taken as equal. The perfect reflection off the surface is accounted for by the boundary condition $\psi_i(z=0) = 0$, while $\psi_i(z \to \infty) = 0$. Position, time, and energy are measured in units of [4]: $z_g = (\hbar^2/2m^2g)^{1/3}$, $t_g = \hbar/E_g$, and $E_g = mgz_g$ (e.g., for neutron: $z_g = 5.87$ μm, $t_g = 1.094$ ms, $E_g = 0.60$ peV). The solutions of Eq. (1) are shifted Airy functions [4]

$$\psi_i(z) = N_i\mathrm{Ai}(z - z_i) = \frac{\mathrm{Ai}(z - z_i)}{|\mathrm{Ai}'(-z_i)|}, \qquad (2)$$

where $-z_i$ are the zeroes of $\mathrm{Ai}(z)$, and $N_i = |\mathrm{Ai}'(-z_i)|^{-1}$ are the normalization constants [65]. The (positive) energies are $E_i = z_i$ [4].

Echo in a classical ensemble of gravitational bouncers.—It is instructive to start from considering the dynamics of $N \gg 1$ classical bouncing particles subject to a pair of delayed pulsed excitations ("kicks"). The first kick initiates nonequilibrium dynamics in the phase space. Here, for clarity of presentation, we model the resulting phase space distribution by a displaced Gaussian with means $\mu_{z,v}$ and variances $\sigma_{z,v}$, for vertical position and velocity [see the bright blue spot in Fig. 1(a)].

Since the classical particle bouncing over an impenetrable reflective surface in the presence of gravity is a nonlinear system, the bouncing frequency of the particle depends on its energy. As a consequence, the initial smooth phase space distribution evolves into a spiral-like structure [see the blue filaments in Fig. 1(a)]. The number of spiral turns increases with time, and they become thinner to conserve the phase-space volume. Such "filamentation" is characteristic of nonlinear systems [51,66,67]. The spiral in the phase space exhibits itself via multiple sharp peaks ("density waves" [68]) in the spatial distribution.

The filamented phase space serves as a basis for the echo formation induced by the second kick applied at $t = t_k$. Depending on the type of QB and specific experimental implementation, various kicking mechanisms can be utilized. As a first example here, we consider particles with nonzero magnetic moment $\boldsymbol{\mu}$, and kick them using pulsed inhomogeneous magnetic field, $\mathbf{B}$. For simplicity, we assume $\mathbf{B}$ has a uniform gradient near the surface [31,32], and fix $\boldsymbol{\mu}$ along or against $\mathbf{B}$. Then, the dimensionless interaction potential is $V_B(z,t) = -s\beta(t)z$ ($s = \pm 1$), $\beta(t) = a_k \exp[-(t - t_k)^2/\sigma_k^2]$, $a_k = |\boldsymbol{\mu}|\hat{\beta}/(mg)$, and $\hat{\beta}$ is the magnitude of the gradient. Figure 1(b) shows the phase space distribution shortly after the kick, leading to particles bunching and formation of localized tips on each branch of the spiral. The filamented structure provides a quasidiscrete set of oscillation frequencies for the tips [55,56], which continue evolving freely and, with time, get out of phase. However, due to their quasidiscrete frequencies, the tips synchronize at twice the delay, at $t \approx 2t_k$ [see Fig. 1(c)], resulting in the echo response [48,51,55,56]. Echo manifests in various physical observables. Here, we consider the average position $\langle z\rangle(t)$ (also averaged over $s = \pm 1$). Figure 1(d) clearly shows the echo response emerging at twice the kick delay, at $t \approx 2t_k$. Although the tips fade with time, they synchronize quasiperiodically producing higher order echoes [51,54,55] visible at $3t_k, 4t_k, \ldots$.

Gravitational wave packet echo.—Initially, the QB is assumed to be in a pure quantum state, e.g., a wave packet of GQSs. A pure GQS has not yet been selected experimentally, due to tunneling of particles through a gravitational barrier [10], but we count on the major reduction of contamination of neighboring GQSs in the future [69]. The QB may be set into motion either by kicking it or by dropping it on the surface from a step [70] or ion trap [24]. We start from the latter and model the initial state by a displaced Gaussian

$$\Psi(z, t=0) = \left(\frac{2}{\pi\sigma_z^2}\right)^{1/4} \exp\left[-\frac{(z-\mu_z)^2}{\sigma_z^2}\right]. \qquad (3)$$

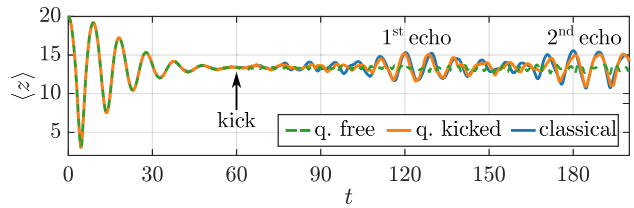

FIG. 2. Echo induced by pulsed inhomogeneous magnetic field kick. The kick is applied at $t = t_k = 60$. Initial state parameters: $\mu_z = 20$, $\sigma_z = 8$ [see Eq. (3)]. Excitation parameters: $a_k = |\boldsymbol{\mu}|\hat{\beta}/mg = 0.5$ (e.g., for neutrons: $\hat{\beta} \approx 0.8$ T/m), and $\sigma_k = 0.5$. The classical result [see Fig. 1(d)] is added for comparison.

This state is similar to the initial phase space distribution used in the classical analysis. In the quantum case, the observable is the expectation value, $\langle z \rangle(t) = \int_0^\infty \Psi^*(z,t) z \Psi(z,t) dz$. In principle, the echo effect can be observed in a variety of experimentally accessible observables, e.g., a flux through the surface [71].

Figure 2 shows that, after several bounces, the wave packet collapses [$\langle z \rangle(t)$ oscillations decay] because of the differences in the transition frequencies of GQSs forming the wave packet (a direct consequence of the anharmonicity of the potential). The echo is induced by a kick applied after a delay t_k. Following the example considered classically, we assume that the QB (an atom, antiatom, or neutron) has spin 1/2 and kick it by a pulsed inhomogeneous magnetic field, $\mathbf{B}$. The Hamiltonian is $H = H_g - s\beta(t)z$, where H_g is defined in Eq. (1), and $s = \pm 1$ corresponds to spin states oriented along or against the field (see the Supplemental Material [72] for details). The echo response is clearly visible at twice the kick delay, at $t \approx 2t_k$. The result is the average of $\langle z \rangle(t)$ obtained for $s = \pm 1$.

The echo of GQSs is conceptually different from classical echoes emerging in ensemble of many nonidentical bouncers. The former can be observed in single bouncers by repeating the experiment many times starting from the same initial state. The interference pattern developing after many measurements is a time-domain analog of the spatial interference fringes formed in the double slit experiment with single electrons (the famous Feynman gedanken experiment, see [73] and references therein). Related echoes have been observed in single atoms interacting with a single mode of cavity [62,63], and in single vibrationally excited molecules [64]. The echo of the GQSs also differs from quantum revivals, which happen in wave packets containing many states without additional kicks. The periodicity of revivals depends only on the energy spectrum [74–77], while the echo period is controlled by the kick delay.

Time-resolved GQS spectroscopy.—An appropriately chosen observable measured as a function of the kick delay contains spectroscopic information about the QB. Here, for example, we choose to follow the population of the ground GQS. The suggested measurement can be realized in the typical flow-through configuration

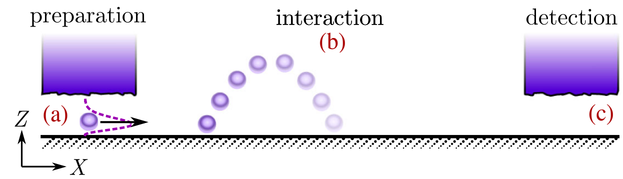

FIG. 3. Schematic of a flow-through experimental setup. Bouncing (along Z axis) particles propagate in X direction. (a) First slit with a rough top surface used for preparation. (b) Interaction region. (c) Second slit used for detection.

(see Fig. 3) [8,27,33,78], or using closed traps for QBs [14,78]. The experiment includes three stages: preparation, interaction, and detection. Initially, particles pass through a narrow slit [(a) in Fig. 3], whose top surface is rough leading to the loss of highly excited particles. A sufficiently long and properly sized slit allows preparing the ground GQS, ψ_1 [79,80]. Then, the QB enters the interaction region [(b) in Fig. 3], where it is subject to two kicks. In the detection stage, the particles pass through the second slit [(c) in Fig. 3] allowing only the population trapped in the ground state to reach the detector (not shown). The delay, τ between the kicks is varied and the population of the ground state is recorded as a function of τ.

For impulsive (and identical) kicks, the Hamiltonian during the excitations is $H \approx V(z)f(t)$. The wave function after the first kick is given by $\Psi_+ = \mathbf{P}\Psi_-$, where Ψ_- is the wave function before the kick, $\mathbf{P} = \exp[-i\alpha V(z)]$, and $\alpha = \int_{-\infty}^{\infty} f(t)dt$. For the initial ground GQS, ψ_1, $\Psi_+ = \sum_{i=1}^\infty P_{i1}\psi_i$, where P_{ij} is the matrix representation of $\mathbf{P}$ in the basis of ψ_is. After a delay τ (just before the second excitation), the wave function is $\Psi_-(\tau) = \sum_{i=1}^\infty P_{i1}\psi_i e^{-iz_i\tau}$. The delay-dependent amplitude of the ground state after the second kick is given by $c_1(\tau) = \sum_{i=1}^\infty P_{1i}^2 \exp[-iz_i\tau]$, while the population reads $|c_1|^2(\tau) = \sum_{i,j=1}^\infty (P_{1i}P_{1j}^*)^2 \exp[-i(z_i - z_j)\tau]$. This signal oscillates at transition frequencies between the GQSs populated by the first kick. The second kick affects the amplitudes of the GQSs but not their transition frequencies. In the limit of weak kicks (keeping only terms with $i = 1$, $j \geq 1$ and $i \geq 1$, $j = 1$) $|c_1|^2(\tau)$ reads

$$|c_1|^2(\tau) \approx \sum_{i=1}^{\infty} (P_{11}^* P_{1i})^2 e^{-i(z_i - z_1)\tau} + \text{c.c.}, \tag{4}$$

where "c.c." stands for complex conjugate. The function in Eq. (4) contains the transition frequencies between the excited states ψ_i and the ground state ψ_1. Notice that the signal contains phase information allowing us, in principle, to retrieve the complex-valued wave function expansion coefficients P_{1i} (up to a π phase). This is analogous to the "quantum holography" procedure [81–84]. The access to phase information may open new possibilities for constraining the parameters of extra interactions [85–88].

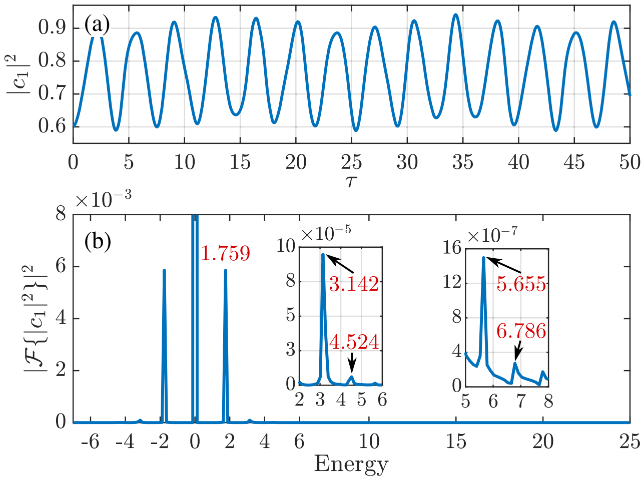

FIG. 4. Time-resolved GQS spectroscopy: kicks by pulsed inhomogeneous magnetic field. (a) $|c_1|^2(\tau)$, kicks' parameters: $a_{k1} = 2$, $a_{k2} = 1$ (e.g., for neutron: $|\boldsymbol{\mu}| = 60.3$ neV/T, $\hat{\beta}_1 \approx 2.4$ T/m, $\hat{\beta}_2 \approx 1.2$ T/m), $\sigma_{k1} = \sigma_{k2} = 0.2$. (b) Spectrum of $|c_1|^2(\tau)$. Peaks correspond to energy differences $\mathcal{E}_{i1}$ ($i = 2, \ldots, 6$). Theoretical energy differences [see Eq. (2)]: $z_{21} = 1.750$, $z_{31} = 3.182$, $z_{41} = 4.449$, $z_{51} = 5.606$, $z_{61} = 6.684$.

Figure 4(a) shows the numerically calculated $|c_1|^2(\tau)$ for the case of two delayed kicks by a pulsed inhomogeneous magnetic field. Here, the time dependence of the field is defined by $\beta(t) = a_{k1} \exp[-t^2/\sigma_{k1}^2] + a_{k2} \exp[-(t-\tau)^2/\sigma_{k2}^2]$. The maximal delay is close to the typical time of flight through the interaction region [(b) in Fig. 3] in experiments with UCNs (see Refs. [8–11,27–29,31–33] for details). Figure 4(b) shows the spectrum of the signal in Fig. 4(a), which mainly contains the energy differences $\mathcal{E}_{ij} = \mathcal{E}_i - \mathcal{E}_j$ between the low-lying excited states ψ_i ($i = 2, \ldots, 6$) and the ground state ψ_1 [see Eq. (4)]. The relative errors defined by $100\% \times (\mathcal{E}_{i1} - z_{i1})/z_{i1}$, where $z_{i1} = z_i - z_1$ [see Eq. (2)], are 0.52%, −1.27%, 1.69%, 0.87%, 1.52% for $i = 2, \ldots, 6$, typical for flow-through experiments. The precision of the extracted frequencies increases with increasing the maximal delay, which can be achieved in closed traps [14]. Moreover, modern digital signal processing techniques [89,90] allow us to significantly increase the spectral resolution compared to the simple Fourier analysis. This is possible by making use of the *a priori* knowledge about the structure of the signal, e.g., the discreteness of its spectrum.

Kick by a jolt from the surface.—Both the wave-packet echoes and the GQS spectroscopy approach discussed above are general and do not depend on the specific type of kicks, as long as they are short. Here, we consider an additional kind of kick caused by a sudden displacement of the reflective boundary. The corresponding Schrödinger equation has a time-dependent boundary condition $\Psi[z = h(t)] = 0$, where $h(t)$ is the mirror surface height (see the Supplemental Material [72] for details). Such a model can, in principle, describe several experimental scenarios in which the kicks are induced by shaking the surface as a whole or by existence of protrusions, grooves, or steps on the surface. Such inhomogeneities appear as a time-dependent boundary in the reference frame copropagating transversally with the QB moving along the surface. Here, $h(t) = a_{k1} \exp[-t^2/\sigma_{k1}^2] + a_{k2} \exp[-(t-\tau)^2/\sigma_{k2}^2]$, where a_{k1}, a_{k2} are the amplitudes of the kicks, and σ_{k1}, σ_{k2} define their widths.

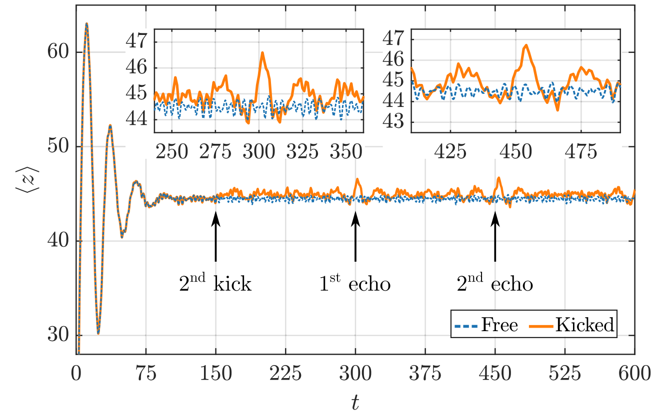

FIG. 5. Echo induced by surface shake. The first kick is applied at $t = 0$, the delay of the second kick is $t_k = 150$. The echo emerges at $t \approx 2t_k, 3t_k$. Kicks' parameters: $a_{k1} = 1.5$, $\sigma_{k1} = 0.1$, $a_{k2} = 1.0$, $\sigma_{k2} = 0.16$.

Figure 5 shows the echo response of $\langle z \rangle(t)$. Here, the QB is initially in the ground state ψ_1. A single kick at $t = 0$ excites a wave packet which collapses after several oscillations (dashed blue). However, when a second kick is applied at $t = t_k$, echo responses emerge at $t \approx 2t_k, 3t_k$ (solid orange).

Figure 6(a) shows $|c_1|^2(\tau)$ in this case, while the corresponding spectrum is shown in Fig. 6(b). The relative

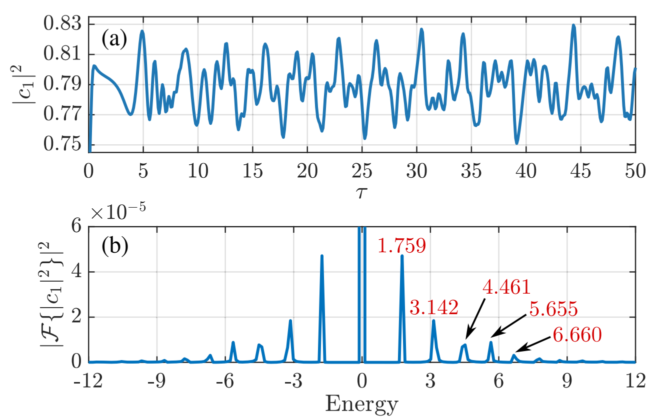

FIG. 6. Time-resolved GQS spectroscopy: kicks by surface shake. (a) $|c_1|^2(\tau)$, kicks' parameters: $a_{k1} = 0.6$, $a_{k2} = 0.1$, and $\sigma_{k1} = \sigma_{k2} = 0.2$. (b) Spectrum of $|c_1|^2(\tau)$ shown in panel (a). Peaks correspond to energy differences $\mathcal{E}_{i1}$ ($i = 2, \ldots, 6$). Theoretical differences [see Eq. (2)]: $z_{21} = 1.750$, $z_{31} = 3.182$, $z_{41} = 4.449$, $z_{51} = 5.606$, $z_{61} = 6.684$, where $z_{i1} = z_i - z_1$.

errors of the extracted energy differences are 0.52%, −1.27%, 0.28%, 0.87%, −0.37% for $i = 2, \ldots, 6$. In the limit of weak kicks ($a_{k1}, a_{k2} \ll 1$), $|c_1|^2(\tau)$ can be obtained using time-dependent perturbation theory [see Eq. (9) in the Supplemental Material [72]]. In agreement with Eq. (4), the signal contains the transition frequencies between the excited states ψ_i and the ground state ψ_1, and the Fourier amplitudes are proportional to the squared expansion coefficients of the wave packet after the first excitation.

Conclusions.—Echo effect in impulsively excited QBs is considered, and the echo formation mechanism is discussed using the auxiliary classical model. Echoes may be used for probing decoherence effects originating from interactions with the environment or other particles. The population of the ground state recorded as a function of the delay is shown to contain the transition frequencies between GQSs excited by the first kick, populations, and partial phases information. The retrieved phases may open opportunities for constraining the parameters of extra fundamental interactions [85–88]. Various initial states, detection schemes, probe particles, and kicking mechanisms can be envisioned for both inducing the echo effect and GQS spectroscopy. This method can be used by the current collaborations working with GQSs of UCNs (Tokyo, qBounce, Los Alamos, GRANIT), with $\bar{\mathrm{H}}$ (GBAR), with hydrogen atoms (GRASIAN), with whispering gallery states of neutrons, atoms, and antiatoms [91].

This work was supported in part by the Israel Science Foundation (Grant No. 746/15). I. A. acknowledges support as the Patricia Elman Bildner Professorial Chair. This research was made possible in part by the historic generosity of the Harold Perlman Family.

*dr.a.voronin@gmail.com
†nesvizhevsky@ill.eu
‡ilya.averbukh@weizmann.ac.il

[1] I. I. Gol'dman, V. D. Krivchenkov, V. I. Kogan, and V. M. Galitskii, *Selected Problems in Quantum Mechanics*, 2nd ed., edited by D. ter Haar (Infosearch Ltd, London, 1964).

[2] P. W. Langhoff, Schrödinger particle in a gravitational well, Am. J. Phys. **39**, 954 (1971).

[3] R. L. Gibbs, The quantum bouncer, Am. J. Phys. **43**, 25 (1975).

[4] J. Gea-Banacloche, A quantum bouncing ball, Am. J. Phys. **67**, 776 (1999).

[5] H. Wallis, J. Dalibard, and C. Cohen-Tannoudji, Trapping atoms in a gravitational cavity, Appl. Phys. B **54**, 407 (1992).

[6] M. F. Andersen, A. Kaplan, N. Friedman, and N. Davidson, Stable islands in chaotic atom-optics billiards, caused by curved trajectories, J. Phys. B **35**, 2183 (2002).

[7] V. V. Nesvizhevsky and A. Voronin, *Surprising Quantum Bounces* (Imperial College Press, London, 2015).

[8] V. V. Nesvizhevsky, H. G. Börner, A. K. Petukhov, H. Abele, S. Baeßler, F. J. Rueß, T. Stöferle, A. Westphal, A. M. Gagarski, G. A. Petrov, and A. V. Strelkov, Quantum states of neutrons in the Earth's gravitational field, Nature (London) **415**, 297 (2002).

[9] V. V. Nesvizhevsky, H. G. Börner, A. M. Gagarski, A. K. Petoukhov, G. A. Petrov, H. Abele, S. Baeßler, G. Divkovic, F. J. Rueß, T. Stöferle, A. Westphal, A. V. Strelkov, K. V. Protasov, and A. Yu. Voronin, Measurement of quantum states of neutrons in the Earth's gravitational field, Phys. Rev. D **67**, 102002 (2003).

[10] V. V. Nesvizhevsky, A. K. Petukhov, H. G. Börner, T. A. Baranova, A. M. Gagarski, G. A. Petrov, K. V. Protasov, A. Yu. Voronin, S. Baeßler, H. Abele, A. Westphal, and L. Lucovac, Study of the neutron quantum states in the gravity field, Eur. Phys. J. C **40**, 479 (2005).

[11] A. Westphal, H. Abele, S. Baeßler, V. V. Nesvizhevsky, K. V. Protasov, and A. Yu. Voronin, A quantum mechanical description of the experiment on the observation of gravitationally bound states, Eur. Phys. J. C **51**, 367 (2007).

[12] V. V. Nesvizhevsky, A. K. Petukhov, K. V. Protasov, and A. Yu. Voronin, Centrifugal quantum states of neutrons, Phys. Rev. A **78**, 033616 (2008).

[13] V. V. Nesvizhevsky, A. Yu. Voronin, R. Cubitt, and K. V. Protasov, Neutron whispering gallery, Nat. Phys. **6**, 114 (2010).

[14] V. V. Nesvizhevsky, F. Nez, S. A. Vasiliev, E. Widmann, P. Crivelli, S. Reynaud, and A. Yu. Voronin, A magneto-gravitational trap for studies of gravitational quantum states, Eur. Phys. J. C **80**, 520 (2020).

[15] A. Yu. Voronin, P. Froelich, and V. V. Nesvizhevsky, Gravitational quantum states of Antihydrogen, Phys. Rev. A **83**, 032903 (2011).

[16] P.-P. Crépin, Quantum reflection of a cold antihydrogen wave packet, Ph.D. thesis, Sorbonne Universites, UPMC University of Paris 6, 2019.

[17] E. G. Adelberger, B. R. Heckel, C. W. Stubbs, and Y. Su, Does Antimatter Fall with the Same Acceleration as Ordinary Matter?, Phys. Rev. Lett. **66**, 850 (1991).

[18] T. W. Darling, F. Rossi, G. I. Opat, and G. F. Moorhead, The fall of charged particles under gravity: A study of experimental problems, Rev. Mod. Phys. **64**, 237 (1992).

[19] F. M. Huber, R. A. Lewis, E. W. Messerschmid, and G. A. Smith, Precision tests of Einstein's weak equivalence principle for antimatter, Adv. Space Res. **25**, 1245 (2000).

[20] C. Amole *et al.* (ALPHA Collaboration), Description and first application of a new technique to measure the gravitational mass of antihydrogen, Nat. Commun. **4**, 1785 (2013).

[21] A. Kellerbauer *et al.*, Proposed antimatter gravity measurement with an antihydrogen beam, Nucl. Instrum. Methods Phys. Res., Sect. B **266**, 351 (2008).

[22] P. Indelicato *et al.*, The GBAR project, or how does antimatter fall?, Hyperfine Interact. **228**, 141 (2014).

[23] W. A. Bertsche, Prospects for comparison of matter and antimatter gravitation with ALPHA-g, Phil. Trans. R. Soc. A **376**, 20170265 (2018).

[24] P.-P. Crépin, C. Christen, R. Guérout, V. V. Nesvizhevsky, A. Yu. Voronin, and S. Reynaud, Quantum interference test

of the equivalence principle on antihydrogen, Phys. Rev. A **99**, 042119 (2019).

[25] V. V. Nesvizhevsky and K. V. Protasov, *Trends in Quantum Gravity Research* (Nova Science Publications, New York, 2006), Chap. Quantum states of neutrons in the Earth's gravitational field: State of the art, applications, perspectives, pp. 65–107.

[26] H. Abele, T. Jenke, H. Leeb, and J. Schmiedmayer, Ramsey's method of separated oscillating fields and its application to gravitationally induced quantum phase shifts, Phys. Rev. D **81**, 065019 (2010).

[27] T. Jenke, P. Geltenbort, H. Lemmel, and H. Abele, Realization of a gravity-resonance-spectroscopy technique, Nat. Phys. **7**, 468 (2011).

[28] T. Jenke, G. Cronenberg, J. Burgdörfer, L. A. Chizhova, P. Geltenbort, A. N. Ivanov, T. Lauer, T. Lins, S. Rotter, H. Saul, U. Schmidt, and H. Abele, Gravity Resonance Spectroscopy Constrains Dark Energy and Dark Matter Scenarios, Phys. Rev. Lett. **112**, 151105 (2014).

[29] G. Cronenberg, P. Brax, H. Filter, P. Geltenbort, T. Jenke, G. Pignol, M. Pitschmann, M. Thalhammer, and H. Abele, Acoustic Rabi oscillations between gravitational quantum states and impact on symmetron dark energy, Nat. Phys. **14**, 1022 (2018).

[30] G. Manfredi, O. Morandi, L. Friedland, T. Jenke, and H. Abele, Chirped-frequency excitation of gravitationally bound ultracold neutrons, Phys. Rev. D **95**, 025016 (2017).

[31] G. Pignol, S. Baeßler, V. V. Nesvizhevsky, K. Protasov, D. Rebreyend, and A. Voronin, Gravitational resonance spectroscopy with an oscillating magnetic field gradient in the GRANIT flow through arrangement, Adv. High Energy Phys. **2014**, 628125 (2014).

[32] S. Baeßler, V. V. Nesvizhevsky, G. Pignol, K. V. Protasov, D. Rebreyend, E. A. Kupriyanova, and A. Yu. Voronin, Frequency shifts in gravitational resonance spectroscopy, Phys. Rev. D **91**, 042006 (2015).

[33] G. Ichikawa, S. Komamiya, Y. Kamiya, Y. Minami, M. Tani, P. Geltenbort, K. Yamamura, M. Nagano, T. Sanuki, S. Kawasaki, M. Hino, and M. Kitaguchi, Observation of the Spatial Distribution of Gravitationally Bound Quantum States of Ultracold Neutrons and Its Derivation Using the Wigner Function, Phys. Rev. Lett. **112**, 071101 (2014).

[34] A. Yu. Voronin, V. V. Nesvizhevsky, O. D. Dalkarov, E. A. Kupriyanova, and P. Froelich, Resonance spectroscopy of gravitational states of antihydrogen, Hyperfine Interact. **228**, 133 (2014).

[35] P.-P. Crépin, G. Dufour, R. Guérout, A. Lambrecht, and S. Reynaud, Casimir-Polder shifts on quantum levitation states, Phys. Rev. A **95**, 032501 (2017).

[36] A. Yu. Voronin, V. V. Nesvizhevsky, G. Dufour, and S. Reynaud, Quantum ballistic experiment on antihydrogen fall, J. Phys. B **49**, 054001 (2016).

[37] V. V. Nesvizhevsky, A. Yu. Voronin, P.-P. Crépin, and S. Reynaud, Interference of several gravitational quantum states of antihydrogen in GBAR experiment, Hyperfine Interact. **240**, 32 (2019).

[38] E. L. Hahn, Spin echoes, Phys. Rev. **80**, 580 (1950).

[39] E. L. Hahn, Free nuclear induction, Phys. Today **6**, 4 (1953).

[40] N. A. Kurnit, I. D. Abella, and S. R. Hartmann, Observation of a Photon Echo, Phys. Rev. Lett. **13**, 567 (1964).

[41] S. Mukamel, *Principles of Nonlinear Optical Spectroscopy* (Oxford University Press, New York, 1995).

[42] R. M. Hill and D. E. Kaplan, Cyclotron Resonance Echo, Phys. Rev. Lett. **14**, 1062 (1965).

[43] R. W. Gould, T. M. O'Neil, and J. H. Malmberg, Plasma Wave Echo, Phys. Rev. Lett. **19**, 219 (1967).

[44] F. Mezei, Neutron spin echo: A new concept in polarized thermal neutron techniques, Z. Phys. A **255**, 146 (1972).

[45] A. Bulatov, A. Kuklov, B. E. Vugmeister, and H. Rabitz, Echo in optical lattices: Stimulated revival of breathing oscillations, Phys. Rev. A **57**, 3788 (1998).

[46] F. B. J. Buchkremer, R. Dumke, H. Levsen, G. Birkl, and W. Ertmer, Wave Packet Echoes in the Motion of Trapped Atoms, Phys. Rev. Lett. **85**, 3121 (2000).

[47] M. Herrera, T. M. Antonsen, E. Ott, and S. Fishman, Echoes and revival echoes in systems of anharmonically confined atoms, Phys. Rev. A **86**, 023613 (2012).

[48] G. Stupakov, Technical Report No. 579, SSC Report No. SSCL-579, SSCL, 1992.

[49] G. V. Stupakov and S. K. Kauffmann, Echo effect in accelerators, Proc. Par. Accel. Conf. **1**, 197 (1993).

[50] L. K. Spentzouris, J.-F. Ostiguy, and P. L. Colestock, Direct Measurement of Diffusion Rates in High Energy Synchrotrons Using Longitudinal Beam Echoes, Phys. Rev. Lett. **76**, 620 (1996).

[51] G. Stupakov, *Handbook of Accelerator Physics and Engineering*, 2nd ed. (World Scientifc, Singapore, 2013), Chap. 2.3.13, pp. 121–123.

[52] T. Sen and Y. S. Li, Nonlinear theory of transverse beam echoes, Phys. Rev. Accel. Beams **21**, 021002 (2018).

[53] G. Karras, E. Hertz, F. Billard, B. Lavorel, J.-M. Hartmann, O. Faucher, E. Gershnabel, Y. Prior, and I. Sh. Averbukh, Orientation and Alignment Echoes, Phys. Rev. Lett. **114**, 153601 (2015).

[54] G. Karras, E. Hertz, F. Billard, B. Lavorel, G. Siour, J.-M. Hartmann, O. Faucher, E. Gershnabel, Y. Prior, and I. Sh. Averbukh, Experimental observation of fractional echoes, Phys. Rev. A **94**, 033404 (2016).

[55] K. Lin, P. Lu, J. Ma, X. Gong, Q. Song, Q. Ji, W. Zhang, H. Zeng, J. Wu, G. Karras, G. Siour, J.-M. Hartmann, O. Faucher, E. Gershnabel, Y. Prior, and I. Sh. Averbukh, Echoes in Space and Time, Phys. Rev. X **6**, 041056 (2016).

[56] K. Lin, I. Tutunnikov, J. Ma, J. Qiang, L. Zhou, O. Faucher, Y. Prior, I. Sh. Averbukh, and J. Wu, Spatiotemporal rotational dynamics of laser-driven molecules, Adv. Opt. Photonics **2**, 1 (2020).

[57] H. Zhang, B. Lavorel, F. Billard, J.-M. Hartmann, E. Hertz, O. Faucher, J. Ma, J. Wu, E. Gershnabel, Y. Prior, and I. Sh. Averbukh, Rotational Echoes as a Tool for Investigating Ultrafast Collisional Dynamics of Molecules, Phys. Rev. Lett. **122**, 193401 (2019).

[58] J. Ma, H. Zhang, B. Lavorel, F. Billard, E. Hertz, J. Wu, C. Boulet, J.-M. Hartmann, and O. Faucher, Observing collisions beyond the secular approximation limit, Nat. Commun. **10**, 5780 (2019).

[59] D. Rosenberg, R. Damari, and S. Fleischer, Echo Spectroscopy in Multilevel Quantum-Mechanical Rotors, Phys. Rev. Lett. **121**, 234101 (2018).

[60] D. Rosenberg and S. Fleischer, Intrinsic calibration of laser-induced molecular alignment using rotational echoes, Phys. Rev. Research **2**, 023351 (2020).
[61] J.-M. Hartmann, J. Ma, T. Delahaye, F. Billard, E. Hertz, J. Wu, B. Lavorel, C. Boulet, and O. Faucher, Molecular alignment echoes probing collision-induced rotational-speed changes, Phys. Rev. Research **2**, 023247 (2020).
[62] G. Morigi, E. Solano, B.-G. Englert, and H. Walther, Measuring irreversible dynamics of a quantum harmonic oscillator, Phys. Rev. A **65**, 040102(R) (2002).
[63] T. Meunier, S. Gleyzes, P. Maioli, A. Auffeves, G. Nogues, M. Brune, J. M. Raimond, and S. Haroche, Rabi Oscillations Revival Induced by Time Reversal: A Test of Mesoscopic Quantum Coherence, Phys. Rev. Lett. **94**, 010401 (2005).
[64] J. Qiang, I. Tutunnikov, P. Lu, K. Lin, W. Zhang, F. Sun, Y. Silberberg, Y. Prior, I. Sh. Averbukh, and J. Wu, Echo in a single vibrationally excited molecule, Nat. Phys. **16**, 328 (2020).
[65] J. R. Albright, Integrals of products of Airy functions, J. Phys. A **10**, 485 (1977).
[66] D. Lynden-Bell, Statistical mechanics of violent relaxation in stellar systems, Mon. Not. R. Astron. Soc. **136**, 101 (1967).
[67] G. Guignard, Phase space dynamics, in *Frontiers of Particle Beams*, edited by M. Month and S. Turner (Springer, Berlin, Heidelberg, 1988), pp. 1–50.
[68] E. J. Kolmes, V. I. Geyko, and N. J. Fisch, Density waves in a system of non-interacting particles, Phys. Lett. A **380**, 3061 (2016).
[69] M. Escobar, F. Lamy, A. E. Meyerovich, and V. V. Nesvizhevsky, Rough mirror as a quantum state selector: Analysis and design, Adv. High Energy Phys. **2014**, 764182 (2014).
[70] V. V. Nesvizhevskii, Investigation of quantum neutron states in the terrestrial gravitational field above a mirror, Phys. Usp. **47**, 515 (2004).
[71] V. V. Nesvizhevsky, R. Cubitt, K. V. Protasov, and A. Yu. Voronin, The whispering gallery effect in neutron scattering, New J. Phys. **12**, 113050 (2010).
[72] See Supplemental Material at http://link.aps.org/supplemental/10.1103/PhysRevLett.126.170403 for the description of our approach to solving the time-dependent Schrödinger equation and derivation of approximate expression for $|c_1|^2(\tau)$.
[73] R. Bach, D. Pope, S.-H. Liou, and H. Batelaan, Controlled double-slit electron diffraction, New J. Phys. **15**, 033018 (2013).
[74] J. H. Eberly, N. B. Narozhny, and J. J. Sanchez-Mondragon, Periodic Spontaneous Collapse and Revival in a Simple Quantum Model, Phys. Rev. Lett. **44**, 1323 (1980).
[75] J. Parker and C. R. Stroud, Coherence and Decay of Rydberg Wave Packets, Phys. Rev. Lett. **56**, 716 (1986).
[76] I. Sh. Averbukh and N. F. Perelman, Fractional revivals: Universality in the long-term evolution of quantum wave packets beyond the correspondence principle dynamics, Phys. Lett. A **139**, 449 (1989).
[77] R. Robinett, Quantum wave packet revivals, Phys. Rep. **392**, 1 (2004).
[78] D. Roulier, F. Vezzu, S. Baeßler, B. Clément, D. Morton, V. V. Nesvizhevsky, G. Pignol, and D. Rebreyend, Status of the GRANIT facility, Adv. High Energy Phys. **2015**, 730437 (2015).
[79] V. I. Luschikov and A. I. Frank, Quantum effects occurring when ultracold neutrons are stored on a plane, JETP Lett. **28**, 559 (1978), http://jetpletters.ru/ps/1579/article_24231.shtml.
[80] V. V. Nesvizhevsky, H. Boerner, A. M. Gagarski, G. A. Petrov, A. K. Petukhov, H. Abele, S. Baessler, T. Stoeferle, and S. M. Soloviev, Search for quantum states of the neutron in a gravitational field: Gravitational levels, Nucl. Instrum. Methods Phys. Res. **440**, 754 (2000).
[81] C. Leichtle, W. P. Schleich, I. Sh. Averbukh, and M. Shapiro, Quantum State Holography, Phys. Rev. Lett. **80**, 1418 (1998).
[82] I. Sh. Averbukh, M. Shapiro, C. Leichtle, and W. P. Schleich, Reconstructing wave packets by quantum-state holography, Phys. Rev. A **59**, 2163 (1999).
[83] T. C. Weinacht, J. Ahn, and P. H. Bucksbaum, Measurement of the Amplitude and Phase of a Sculpted Rydberg Wave Packet, Phys. Rev. Lett. **80**, 5508 (1998).
[84] T. C. Weinacht, J. Ahn, and P. H. Bucksbaum, Controlling the shape of a quantum wave function, Nature (London) **397**, 233 (1999).
[85] H. Abele, S. Baeßler, and A. Westphal, Quantum states of neutrons in the gravitational field and limits for non-newtonian interaction in the range between 1 μm and 10 μm, in *Quantum Gravity: From Theory to Experimental Search*, edited by D. J. W. Giulini, C. Kiefer, and C. Lämmerzahl (Springer, Berlin, Heidelberg, 2003), pp. 355–366.
[86] S. Baeßler, V. V. Nesvizhevsky, K. V. Protasov, and A. Yu. Voronin, Constraint on the coupling of axionlike particles to matter via an ultracold neutron gravitational experiment, Phys. Rev. D **75**, 075006 (2007).
[87] I. Antoniadis, S. Baessler, M. Büchner, V. V. Fedorov, S. Hoedl, A. Lambrecht, V. V. Nesvizhevsky, G. Pignol, K. V. Protasov, S. Reynaud, and Y. Sobolev, Short-range fundamental forces, C.R. Phys. **12**, 755 (2011).
[88] P. Brax and G. Pignol, Strongly Coupled Chameleons and the Neutronic Quantum Bouncer, Phys. Rev. Lett. **107**, 111301 (2011).
[89] P. Stoica and R. Moses, *Spectral Analysis of Signals* (Prentice Hall, Upper Saddle River, 2005).
[90] T. P. Zielinski, *Starting Digital Signal Processing in Telecommunication Engineering*, 1st ed. (Springer International Publishing, New York, 2021).
[91] S. Vasiliev, J. Ahokas, J. Järvinen, V. Nesvizhevsky, A. Voronin, F. Nez, and S. Reynaud, Gravitational and matter-wave spectroscopy of atomic hydrogen at ultra-low energies, Hyperfine Interact. **240**, 14 (2019).